Title
Annotating STEAP1 Regulation in Prostate Cancer with 89Zr Immuno-PET

Journal
Journal of Nuclear Medicine, 55(12)

ISSN
0161-5505

Authors
Doran, Michael G
Watson, Philip A
Cheal, Sarah M
et al.

Publication Date
2014-12-01

DOI
10.2967/jnumed.114.145185

Peer reviewed

HHS Public Access

Author manuscript

J Nucl Med. Author manuscript; available in PMC 2015 April 27.

Published in final edited form as:

J Nucl Med. 2014 December ; 55(12): 2045–2049. doi:10.2967/jnumed.114.145185.

Annotating STEAP1 Regulation in Prostate Cancer with ^{89}Zr Immuno-PET

Michael G. Doran[1,*], **Philip A. Watson**[2,*], **Sarah M. Cheal**[1], **Daniel E. Spratt**[3], **John Wongvipat**[2], **Jeffrey M. Steckler**[2], **Jorge A. Carrasquillo**[1], **Michael J. Evans**[2], and **Jason S. Lewis**[1,4]

[1]Department of Radiology, Memorial Sloan Kettering Cancer Center, New York, New York

[2]Human Oncology and Pathogenesis Program, Memorial Sloan Kettering Cancer Center, New York, New York

[3]Department of Radiation Oncology, Memorial Sloan Kettering Cancer Center, New York, New York

[4]Molecular Pharmacology and Chemistry Program, Memorial Sloan Kettering Cancer Center, New York, New York

Abstract

Antibodies and antibody-drug conjugates targeting the cell surface protein 6 transmembrane epithelial antigen of prostate 1 (STEAP1) are in early clinical development for the treatment of castration-resistant prostate cancer (PCa). In general, antigen expression directly affects the bioactivity of therapeutic antibodies, and the biologic regulation of STEAP1 is unusually complicated in PCa. Paradoxically, STEAP1 can be induced or repressed by the androgen receptor (AR) in different human PCa models, while also expressed in AR-null PCa. Consequently, there is an urgent need to translate diagnostic strategies to establish which regulatory mechanism predominates in patients to situate the appropriate therapy within standard of care therapies inhibiting AR.

Methods—To this end, we prepared and evaluated ^{89}Zr-labeled MSTP2109A (^{89}Zr-2109A), a radiotracer for PET derived from a fully humanized monoclonal antibody to STEAP1 in preclinical PCa models.

For correspondence or reprints contact either of the following: Michael J. Evans, Department of Radiology and Biomedical Imaging, University of California, San Francisco, 185 Berry St., Lobby 6, Suite 350, San Francisco, CA 94143-0946. michael.evans@ucsf.edu. Jason S. Lewis, Department of Radiology, Memorial Sloan Kettering Cancer Center, 1275 York Ave., Box 20, New York, NY 10065. lewisj2@mskcc.org.

*Contributed equally to this work.

DISCLOSURE

Financial support for this study was provided by the following: the Imaging and Radiation Sciences Bridge Program of MSKCC; the Radiological Society of North America 2013 Research Resident grant (#RR1350); the 2014 Prostate Cancer Foundation Young Investigator Award; a David H. Koch Young Investigator Award from the Prostate Cancer Foundation; the National Institutes of Health (NIH) (1K99CA172605-01, 1R01CA17661-01); the NIH Shared Instrumentation grant S10 RR020892-01, which provided funding support for the purchase of the Focus 120 microPET; and the NIH Cancer Center Support grant P30CA008748-48. No other potential conflicts of interest relevant to this article are reported.

Results—^{89}Zr-2109A specifically localized to the STEAP1-positive human PCa models CWR22Pc, 22Rv1, and PC3. Moreover, ^{89}Zr-2109A sensitively measured treatment-induced changes (~66% decline) in STEAP1 expression in CWR22PC in vitro and in vivo, a model we showed to express STEAP1 in an AR-dependent manner.

Conclusion—These findings highlight the ability of immuno-PET with ^{89}Zr-2109A to detect acute changes in STEAP1 expression and argue for an expansion of ongoing efforts to image PCa patients with ^{89}Zr-2109A to maximize the clinical benefit associated with antibodies or antibody-drug conjugates to STEAP1.

Keywords

PET; prostate cancer; androgen receptor

On the basis of its upregulation in several contexts, the cell surface protein 6 transmembrane epithelial antigen of prostate 1 (STEAP1) has been the focus of multiple antibody development programs for therapy (1,2). The most mature technology is MSTP2109A, a fully humanized monoclonal antibody targeting an extracellular epitope. 2109A is under early clinical evaluation for the treatment of castration-resistant prostate cancer (CRPC) as an antibody-drug conjugate termed DSTP3086S (NCT01283373).

To better understand the in vivo properties of DSTP3086S, a companion imaging trial with a ^{89}Zr-labeled adduct of 2109A for PET was simultaneously opened at Memorial Sloan Kettering Cancer Center (MSKCC) for patients with CRPC (NCT01774071). The primary endpoint of this trial was to determine safety and ability to detect sites of metastatic prostate cancer as well as pharmacokinetics and biodistribution of the systemically administered radiotracer.

On the basis of these considerations, we considered it timely to revisit preclinical prostate cancer (PCa) models to explore additional applications for ^{89}Zr-2109A PET in the management of CRPC. Because STEAP1 can be an androgen-regulated gene, we felt one immediately obvious application to consider was the use of ^{89}Zr-2109A PET to monitor the impact of antiandrogen therapy on its expression. Indeed, we have previously disclosed two readily translatable immuno-PET strategies for measuring androgen receptor (AR) signaling by targeting gene products transcriptionally regulated by AR (3–5).

Although our prior immuno-PET strategies were intended to assess antiandrogen pharmacodynamics, our rationale for studying STEAP1 expression changes induced by antiandrogen therapy is slightly different. Paradoxically, STEAP1 expression can be androgen-stimulated, androgen-repressed, or androgen-independent in pre-clinical PCa models (6–11). Because of the limited breadth of PCa models, it is challenging to extrapolate which mechanism predominates in clinical disease. Understanding this could have immediate implications for how DSTP3086S is applied in patients. For instance, should STEAP1 prove to be most commonly androgen-repressed or androgen-independent in clinical disease, DSTP3086S could likely be immediately applied in combination with standard-of-care antiandrogen therapy to improve survival benefit.

In this regard, the purpose of this study was to investigate whether ^{89}Zr-2109A could measure treatment-induced changes in STEAP1 expression in preclinical PCa models. We anticipated these data would empower a trial profiling a larger population of patients to better define this aspect of STEAP1 biology.

MATERIALS AND METHODS

General Methods

The human PCa cell line CWR22Pc was a generous gift from Marja Nevalainen of Thomas Jefferson University and cultured according to the previously disclosed protocol (12). CWR22Rv1, PC3, and HEK293T were purchased from American Type Culture Collection and cultured according to the manufacturer's instructions. Antibodies to AR (sc-816; Santa Cruz Biotechnology), FKBP5 (AF4094; R&D Systems), glyceraldehyde-3-phosphate dehydrogenase (ab9485; Abcam), PMEPA1 (WH0056937M1-100UG; Sigma-Aldrich), SGK (3272; Cell Signaling Technology), and STEAP1 (sc-271872; Santa Cruz Biotechnology) were purchased and used according to the manufacturer's instructions. The mouse monoclonal antibody to prostate-specific membrane antigen (13D6) was the generous gift of Dr. Polly Gregor at MSKCC.

Radiosynthesis of ^{89}Zr-2109A

The antibody MSTP2109A was provided by Genentech. Desferrioxamine B was conjugated to lysine residues via succinimidyl esters as previously described (13). The radiolabeling was performed in neutral buffers at room temperature for 1 h, resulting in a specific activity of approximately 11.1 MBq/mg and a radiochemical yield of greater than 80%. Radiochemical purity was greater than 99% as determined by instant thin-layer chromatography using a running buffer of 5 mM diethylenetriaminepentaacetic acid, pH 5.

Lindmo Assay

A complementary DNA encoding full-length human STEAP1 was purchased (Open Biosystems) and transiently transfected into 1×10^7 HEK293T cells using Lipofectamine 2000 (Invitrogen). The overexpression of the protein was confirmed by immunoblot of whole-cell lysates 72 h after transfection. A separate treatment arm was reserved for the Lindmo assay. Starting with 2.5×10^6 cells, a range of dilutions was assayed for antigen binding by incubation with radiolabeled antibody for 1 h at room temperature. The cell-bound and unbound activity was manually partitioned and assayed with a γ counter. The percentage of bound activity was plotted against the reciprocal of the cell concentration, and a linear regression was used to determine the *y*-intercept (i.e., immunoreactive percentage of the antibody lot).

Generation of CWR22Pc Sublines with Stable AR Suppression

CWR22Pc cells were infected with lentiviral AR short hairpin (shRNA) particles from the MISSION TRC shRNA collection (Sigma-Aldrich) at a multiplicity of infection equal to 3 and selected with puromycin for 8 d, and then whole cell lysates were collected using M-PER protein extraction reagent (Pierce). shRNA reagents used in this study were TRCN0000003715 (shRNA-1), TRCN0000003717 (shRNA-2), TRCN0000003718

(shRNA-3), TRCN0000314730 (shRNA-4), TRCN0000350462 (shRNA-5), and the nonmammalian, nontargeting shRNA control (SHC202V).

Cell Proliferation Assays

Cells were counted and seeded in 12-well plates (0.1×10^6 per well) 18 h before the initiation of drug treatment (vehicle or enzalutamide or ARN-509 at 10 μM). At 2 and 5 d, cells were washed and trypsinized. Viable cells were determined with a trypan blue exclusion assay.

Animal Studies

All animal studies were conducted in compliance with the Research Animal Resource Center guidelines at MSKCC. Three- to 5-wk-old male CB-17 severe combined immunodeficiency mice were obtained from Taconic Farms. The animals weighed approximately 20–25 g. Approximately 1×10^6 human prostate cancer cells were injected subcutaneously into one or both flanks of intact male mice in a 1:1 mixture (v/v) of medium and Matrigel (BD Biosciences). Tumors became palpable within 3–6 wk. Enzalutamide was prepared for dosing with a final dimethyl sulfoxide concentration of 5%, and vehicle was 1% carboxymethyl cellulose, 0/1% polysorbate 80, and 5% dimethyl sulfoxide. Vehicle or enzalutamide was given daily by oral gavage. Tumors were processed for either protein or RNA. Protein expression was analyzed by immunoblot. RNA was converted to complementary DNA and analyzed by quantification polymerase chain reaction for messenger RNA (mRNA) expression. Tumor volume measurements were determined with caliper measurements of the dimensions (width × length × height).

Small-Animal PET Imaging

PET was conducted using a Focus 120 micro-PET scanner (Siemens). Mice were injected with 11.1–12.95 MBq of ^{89}Zr-2109A via the tail vein. While anesthetized with 2% isoflurane, the mice were imaged at various time points (1, 4, 8, 24, 48, 120, and 168 h after injection). Images were acquired within an energy window of 350–750 keV and a coincidence-timing window of 6 ns. Mice were imaged for the time necessary to record 20 million coincident events. The data were converted into 2-dimensional histograms, and images were reconstructed by filtered backprojection.

Biodistribution Studies

To evaluate the uptake of ^{89}Zr-2109A in human PCa xenografts, biodistribution studies were conducted. After tumors grew to approximately 200 mm^3, mice received 2.77–3.7 MBq of ^{89}Zr-2109A via tail vein injection. Animals (n = 5) were humanely euthanized by CO_2 asphyxiation at 1, 4, 8, 24, 48, 120, and 168 h after injection. Blood and 13 organs were harvested immediately after sacrifice. The organs were the heart, lung, liver, kidney, spleen, stomach, large intestine, small intestine, bone, muscle, skin, pancreas, and brain. The tissues were weighed and counted using a γ counter to measure incorporation of ^{89}Zr. Calibration with known amounts of ^{89}Zr was performed to determine the amount of activity in each organ. The activity in each organ was decay-corrected, and the percentage injected dose per gram of tissue was calculated and reported.

Statistical Analysis

Data were analyzed using the unpaired, 2-tailed Student *t* test. Differences at the 95% confidence level ($P < 0.05$) were considered to be statistically significant.

RESULTS

^{89}Zr-2109A Is Specifically Bound by Human PCa Models In Vitro and In Vivo

^{89}Zr-2109A was radiolabeled using routine bioconjugation chemistry to append desferrioxamine B to the antibody, and incubation with ^{89}Zr oxalate at room temperature for 1 h afforded high radiochemical yields of the construct. A binding assay in HEK293T cells transiently overexpressing full-length human STEAP1 showed approximately 85% of the radiolabeled lot to be immunoreactive for STEAP1 (Supplemental Fig. 1; supplemental materials are available at http://jnm.snmjournals.org).

We next conducted proof-of-concept imaging studies in intact male mice inoculated subcutaneously with CWR22Pc cells, an AR-positive human PCa model we had previously shown to abundantly express STEAP1. Evidence of specific tumor uptake was observed within 4 h and persisted for 168 h (Fig. 1A). The companion biodistribution study corroborated this trend, and the accumulation of ^{89}Zr-2109A in the tumor exceeded the activity in the blood after 24 h. Maximal intratumoral activity was observed at 120 h (Fig. 1B; Supplemental Fig. 2). Retention of the radiotracer was generally low in normal tissues, or depleted over time, with the notable exception of the spleen. Encouragingly, little accumulation of activity was observed in the bone (a target of certain free Zr^{4+} salts) (14), suggesting minimal radiotracer degradation in vivo.

To determine the specificity of ^{89}Zr-2109A binding, we coinjected ^{89}Zr-2109A and a 1,000-fold excess of unlabeled 2109A (Fig. 1C; Supplemental Fig. 3). At 24 h, there was a significant reduction in tumor activity, whereas normal tissues with abundant activity were not affected by the unlabeled antibody. Consistent with these findings, little ^{89}Zr-2109A was observed by PET or biodistribution studies in CWR22Rv1 or PC3 tumors, 2 human PCa models we showed to express substantially lower STEAP1 protein in vivo (Fig. 1C; Supplemental Figs. 4–7). Collectively, these findings support the specific interaction between ^{89}Zr-2109A and its antigen on STEAP1 in complex biologic systems.

STEAP1 Expression Is Regulated by AR in CWR22Pc Cells In Vitro and In Vivo

Because CWR22Pc is an AR-positive human PCa model whose growth is inhibited by androgen depletion, we next asked whether and how AR ablation/inhibition affected STEAP1 expression. We first stably transduced the cell line with 5 discrete shRNAs to full-length AR or a nontargeting shRNA to evaluate the impact of AR ablation on STEAP1 expression. Western blotting confirmed knockdown of full-length AR in shRNA-1, -3, and -5 (Fig. 2A). Among these shRNA, only shRNA-2 recognizes an mRNA target site contained within both the full-length AR and the AR splice variant, AR-V7 (15). As with other known AR target genes, STEAP1 was downregulated with knockdown of the full-length AR (Fig. 2A; Supplemental Fig. 8). To corroborate this finding pharmacologically, we treated CWR22Pc with bioactive doses of enzalutamide and ARN-509, standard-of-care

and experimental antiandrogens, respectively (Supplemental Fig. 9) (16,17). Consistent with the shRNA data, pharmacologic inhibition of AR also repressed STEAP1 mRNA and protein (Supplemental Figs. 10 and 11).

We next defined experimental parameters to test androgen regulation of STEAP1 in vivo. Tumor-bearing intact mice were subjected to treatment with vehicle, orchiectomy, or orchiectomy and enzalutamide (30 mg/kg). Following the tumor growth for 28 d showed a steady increase in the vehicle-treatment arm, a lag in tumor growth affected by orchiectomy, and tumor regression in the treatment arm receiving antiandrogen therapy after orchiectomy (Fig. 2B).

We applied these experimental conditions to a separate cohort of animals to determine whether STEAP1 expression is acutely affected by therapies suppressing AR activity. Significant reductions in STEAP1 mRNA levels (Fig. 2C) accompanied by visibly obvious changes in STEAP1 protein (Fig. 2D) were observed in both orchiectomy and orchiectomy combined with enzalutamide after 7 d (a time point in which no changes in tumor volume are evident). Intriguingly, enzalutamide did not significantly reduce STEAP1 levels, a phenomenon perhaps attributable to competition for AR ligand binding sites with high levels of endogenous circulating androgen. Single-agent enzalutamide therapy minimally affected TMPRSS2 mRNA levels, whereas orchiectomy suppressed TMPRSS2 (Supplemental Fig. 12).

^{89}Zr-2109A Quantitatively Measures Pharmacologically Induced Changes in STEAP1 Expression In Vivo

To determine whether these expression changes were large enough to be quantified with ^{89}Zr-2109A, intact male mice were inoculated with bilateral subcutaneous CWR22Pc tumors. Seven days after orchiectomy (or no treatment), a posttherapy PET scan was conducted, and region-of-interest analysis showed an approximately 66% lower intensity signal at the site of the tumor in the orchiectomy group (Figs. 3A and 3B; Supplemental Fig. 13). A biodistribution study was also conducted for selected tissues (Fig. 3C). Tissue activity was significantly lower in the tumors derived from orchiectomized mice than intact mice. There were no significant differences in tissue activity in blood, muscle, or bone between treatment arms.

DISCUSSION

In this study, we report the first evidence, to our knowledge, that treatment-induced regulation of STEAP1 expression can be quantitatively measured with ^{89}Zr-2109A PET in a human PCa model. We established proof of concept by exposing CWR22Pc, a hormone-dependent human PCa model that harbors AR-regulated STEAP1 expression, to orchiectomy in a mouse. These data, combined with the recent progress advancing DSTP3086S into the clinic, press for an expansion of the ongoing effort to quantitate STEAP1 expression levels in patients with ^{89}Zr-2109A PET to explore the potential opportunity for combination therapy with an antiandrogen.

To date, the most visible roles for immuno-PET have been determining the pharmacokinetics of the therapeutic agent, estimating dosimetry for radiotherapy, or identifying up front patients whose tumors harbor high antigen expression (18). A less discussed application whose importance we feel is underscored by this study is using immuno-PET to assess antigen expression changes induced by standard-of-care therapies that might be attractive to combine with the cognate antibody-drug conjugate. PCa is a malignancy for which this application seems particularly germane for at least three reasons. First, patients with CRPC have endured and failed several years of chemical castration, antiandrogens, and cytotoxic chemotherapy. Escape from these chronic treatment pressures promotes diverse evolutionary changes, highlighted by recent molecular profiles of large-scale CRPC biopsy series demonstrating immense genomic instability (19–21). Second, there is compelling and abundant clinical evidence showing improved local control/outcomes with combination therapies (22–24), a finding that has stimulated discussion toward analogous studies in CRPC (25). Third, the limited breadth of PCa models notoriously stifles the discovery of clinically relevant biology or the confident prediction of incidence in clinical disease. In this regard, there are sound rationales to study the impact of standard of care on antigen expression directly in patients with a translational technology such as immuno-PET.

How STEAP1 is regulated in PCa is not well understood in any context. That STEAP1 mRNA levels are suppressed by genetically or pharmacologically inhibiting AR suggests an AR/STEAP1 interaction at the level of transcription. Intriguingly, we and others (26) have generated ChIP-seq data for LNCaP or LNCaP-AR, and an examination of these data revealed no compelling evidence of AR-binding peaks within or immediately around the STEAP1 gene (data not shown). However, STEAP1 is AR-repressed in these models, and we are actively pursuing ChIP-seq studies with CWR22Pc to better understand how AR might regulate STEAP1 in a genetic background in which STEAP1 is androgen-stimulated.

These considerations further underscore the growing appreciation that “castration-resistant PCa” is an umbrella term encompassing many molecularly distinct malignancies. That a drug target such as STEAP1 is so differentially regulated by standard-of-care therapy makes an especially urgent case for immuno-PET as a companion diagnostic to an antibody-drug conjugate, and given that the imaging trial is being performed concurrently with the therapy trial, there is a realistic opportunity to demonstrate the virtues of ^{89}Zr-2109A to encourage its commercialization.

CONCLUSION

These findings highlight the ability of immuno-PET with ^{89}Zr-2109A to detect acute changes in STEAP1 expression and argue for an expansion of ongoing efforts to image PCa patients with ^{89}Zr-2109A to maximize the clinical benefit associated with antibodies or antibody-drug conjugates to STEAP1.

Supplementary Material

Refer to Web version on PubMed Central for supplementary material.

Acknowledgments

We acknowledge Drs. Charles Sawyers, Brett Carver, Steven Larson, and Nagavarakishore Pillarsetty for constructive discussions and Valerie Longo and Dr. Pat Zanzonico of the Small Animal Imaging Core at MSKCC for technical assistance. Technical services provided by the MSKCC Small-Animal Imaging Core Facility and the MSKCC Radiochemistry & Molecular Imaging Probe Core are gratefully acknowledged.

References

1. Boswell CA, Mundo EE, Zhang C, et al. Impact of drug conjugation on pharmacokinetics and tissue distribution of anti-STEAP1 antibody-drug conjugates in rats. Bioconjug Chem. 2011; 22:1994–2004. [PubMed: 21913715]
2. Challita-Eid PM, Morrison K, Etessami S, et al. Monoclonal antibodies to six-transmembrane epithelial antigen of the prostate-1 inhibit intercellular communication in vitro and growth of human tumor xenografts in vivo. Cancer Res. 2007; 67:5798–5805. [PubMed: 17575147]
3. Ulmert D, Evans MJ, Holland JP, et al. Imaging androgen receptor signaling with a radiotracer targeting free prostate-specific antigen. Cancer Discov. 2012; 2:320–327. [PubMed: 22576209]
4. Evans MJ, Smith-Jones PM, Wongvipat J, et al. Noninvasive measurement of androgen receptor signaling with a positron-emitting radiopharmaceutical that targets prostate-specific membrane antigen. Proc Natl Acad Sci USA. 2011; 108:9578–9582. [PubMed: 21606347]
5. Evans MJ. Measuring oncogenic signaling pathways in cancer with PET: an emerging paradigm from studies in castration-resistant prostate cancer. Cancer Discov. 2012; 2:985–994. [PubMed: 23043150]
6. Marques RB, Dits NF, Erkens-Schulze S, van Weerden WM, Jenster G. Bypass mechanisms of the androgen receptor pathway in therapy-resistant prostate cancer cell models. PLoS ONE. 2010; 5:e13500. [PubMed: 20976069]
7. Marques RB, Dits NF, Erkens-Schulze S, van Ijcken WF, van Weerden WM, Jenster G. Modulation of androgen receptor signaling in hormonal therapy-resistant prostate cancer cell lines. PLoS ONE. 2011; 6:e23144. [PubMed: 21829708]
8. Gomes IM, Santos CR, Socorro S, Maia CJ. Six transmembrane epithelial antigen of the prostate 1 is down-regulated by sex hormones in prostate cells. Prostate. 2013; 73:605–613. [PubMed: 23060075]
9. Hubert RS, Vivanco I, Chen E, et al. STEAP: a prostate-specific cell-surface antigen highly expressed in human prostate tumors. Proc Natl Acad Sci USA. 1999; 96:14523–14528. [PubMed: 10588738]
10. Moreaux J, Kassambara A, Hose D, Klein B. STEAP1 is overexpressed in cancers: a promising therapeutic target. Biochem Biophys Res Commun. 2012; 429:148–155. [PubMed: 23142226]
11. Gomes IM, Arinto P, Lopes C, Santos CR, Maia CJ. STEAP1 is overexpressed in prostate cancer and prostatic intraepithelial neoplasia lesions, and it is positively associated with Gleason score. Urol Oncol. 2014; 32:53 e23–e59. [PubMed: 24239460]
12. Dagvadorj A, Tan SH, Liao Z, Cavalli LR, Haddad BR, Nevalainen MT. Androgen-regulated and highly tumorigenic human prostate cancer cell line established from a transplantable primary CWR22 tumor. Clin Can Res. 2008; 14:6062–6072.
13. Holland JP, Divilov V, Bander NH, Smith-Jones PM, Larson SM, Lewis JS. ^{89}Zr-DFO-J591 for immunoPET of prostate-specific membrane antigen expression in vivo. J Nucl Med. 2010; 51:1293–1300. [PubMed: 20660376]
14. Holland JP, Sheh Y, Lewis JS. Standardized methods for the production of high specific-activity zirconium-89. Nucl Med Biol. 2009; 36:729–739. [PubMed: 19720285]
15. Hu R, Dunn TA, Wei S, et al. Ligand-independent androgen receptor variants derived from splicing of cryptic exons signify hormone-refractory prostate cancer. Cancer Res. 2009; 69:16–22. [PubMed: 19117982]
16. Tran C, Ouk S, Clegg NJ, et al. Development of a second-generation antiandrogen for treatment of advanced prostate cancer. Science. 2009; 324:787–790. [PubMed: 19359544]

17. Clegg NJ, Wongvipat J, Joseph JD, et al. ARN-509: a novel antiandrogen for prostate cancer treatment. Cancer Res. 2012; 72:1494–1503. [PubMed: 22266222]
18. Knowles SM, Wu AM. Advances in immunopositron emission tomography: antibodies for molecular imaging in oncology. J Clin Oncol. 2012; 30:3884–3892. [PubMed: 22987087]
19. Taylor BS, Schultz N, Hieronymus H, et al. Integrative genomic profiling of human prostate cancer. Cancer Cell. 2010; 18:11–22. [PubMed: 20579941]
20. Shah RB, Mehra R, Chinnaiyan AM, et al. Androgen-independent prostate cancer is a heterogeneous group of diseases: lessons from a rapid autopsy program. Cancer Res. 2004; 64:9209–9216. [PubMed: 15604294]
21. Mehra R, Kumar-Sinha C, Shankar S, et al. Characterization of bone metastases from rapid autopsies of prostate cancer patients. Clin Cancer Res. 2011; 17:3924–3932. [PubMed: 21555375]
22. Roach M 3rd. Current trends for the use of androgen deprivation therapy in conjunction with radiotherapy for patients with unfavorable intermediate-risk, high-risk, localized, and locally advanced prostate cancer. Cancer. 2014; 120:1620–1629. [PubMed: 24591080]
23. Zumsteg ZS, Spratt DE, Pei X, et al. Short-term androgen-deprivation therapy improves prostate cancer-specific mortality in intermediate-risk prostate cancer patients undergoing dose-escalated external beam radiation therapy. Int J Radiat Oncol Biol Phys. 2013; 85:1012–1017. [PubMed: 22981709]
24. Jones CU, Hunt D, McGowan DG, et al. Radiotherapy and short-term androgen deprivation for localized prostate cancer. N Engl J Med. 2011; 365:107–118. [PubMed: 21751904]
25. Glickman MS, Sawyers CL. Converting cancer therapies into cures: lessons from infectious diseases. Cell. 2012; 148:1089–1098. [PubMed: 22424221]
26. Yu J, Yu J, Mani RS, et al. An integrated network of androgen receptor, polycomb, and TMPRSS2-ERG gene fusions in prostate cancer progression. Cancer Cell. 2010; 17:443–454. [PubMed: 20478527]

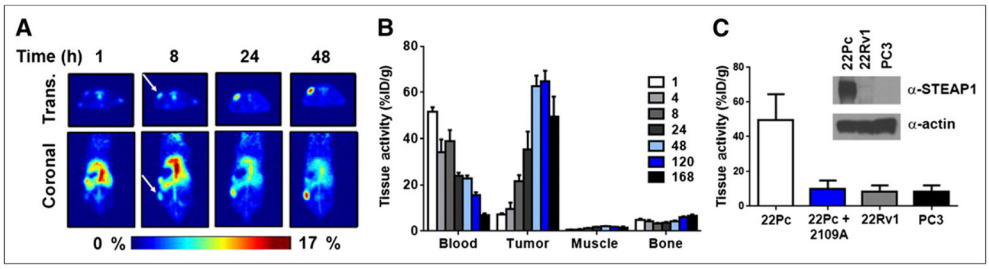

FIGURE 1.

^{89}Zr-2109A specifically targets human PCa xenografts in vivo. (A) Representative coronal and transverse slices of intact male mice harboring CWR22Pc tumors (n = 5) show onset of ^{89}Zr-2109A accumulation at tumor over time. Arrows indicate position of subcutaneous tumor. (B) Biodistribution data (n = 5/time point) for selected tissues over full time course of study show rate of clearance from circulation, and accumulation at tumor, for ^{89}Zr-2109A. There is minimal uptake of radiotracer in muscle, as well as little activity in bone, even at later time points during which radiotracer metabolism can result in free $^{89}Zr^{4+}$ salts. (C) Summary of tumor-associated activity of ^{89}Zr-2109A shows suppression with excess cold antibody (^{89}Zr-2109A + 2109A) and low uptake in human PCa xenografts expressing little to no detectable STEAP1 protein. Inset shows representative immunoblot of relative expression of STEAP1 in models used in this study. %ID/g = percentage injected dose per gram; Trans. = transverse.

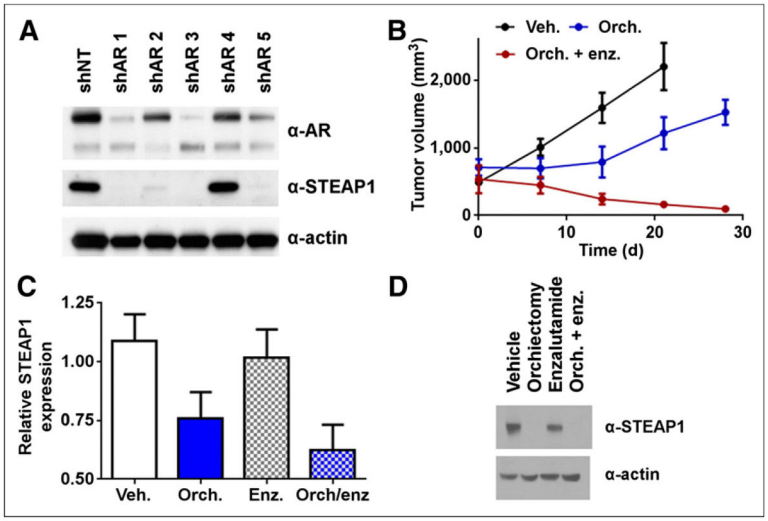

FIGURE 2.

Genetic or pharmacologic inhibition of AR suppresses STEAP1 expression in CWR22Pc. (A) Stable suppression of AR with shRNA results in suppression of STEAP1 protein. CWR22Pc cells were transduced with 1 of 5 pools of lentiviral particles harboring discrete hairpins to AR (shAR1–5) or nontargeting hairpin (shNT). Cell lysates were collected from stable lines after puromycin selection for immunoblotting. AR was potently downregulated with concomitant suppression of STEAP1 protein. Data are representative of 3 independent experiments. (B) Intact animals (n = 5/treatment arm) bearing CWR22Pc tumors were treated with vehicle (veh.), orchiectomy (orch.), or orchiectomy with subsequent daily oral gavage of enzalutamide (enz.) (30 mg/kg). Tumor volume measurements showed that orchiectomy reduced rate of tumor growth, compared with vehicle, and combination therapy resulted in tumor regression over 28 d. (C) Representative immunoblot from CWR22Pc xenografts treated for 7 d shows that orchiectomy alone or orchiectomy + enzalutamide results in dramatic reduction of STEAP1 expression.

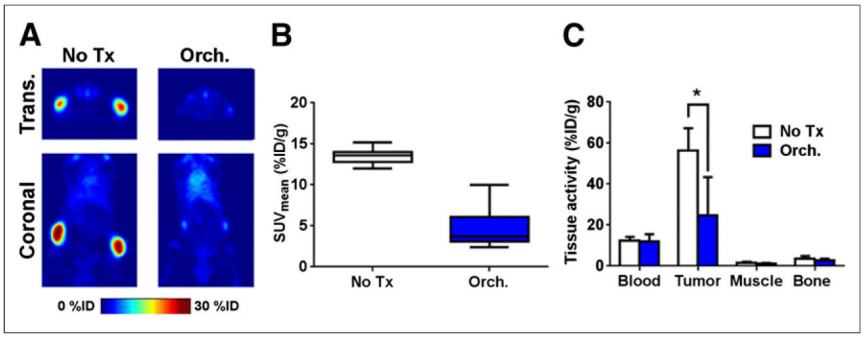

FIGURE 3.

^{89}Zr-2109A quantitatively measures STEAP1 expression changes triggered by androgen-deprivation therapy. (A) Representative coronal and transverse slices of PET data collected from intact male mice bearing CWR22Pc xenografts (n = 5). Animals receiving orchiectomy (orch.) harbored tumors with significantly less radiotracer uptake than those receiving no treatment (no tx) 9 d after surgical manipulation. Radiotracer was injected on day 7, and images were acquired 48 h after injection of ^{89}Zr-2109A. (B) Graphical representation of mean standardized uptake values for tumors from each treatment arm shows downregulation of ^{89}Zr-2109A uptake in tumor by orchiectomy. (C) Biodistribution data from selected tissues, collected 48 h after injection of radiotracer, show significant reduction in tumor uptake in orchiectomy treatment arm. Biodistribution values for blood, muscle, and bone were consistent with what was previously determined in pilot study. *P < 0.01. %ID/g = percentage injected dose per gram; Trans. = transverse.